

Paleoflooding in the Solar System: comparison among mechanisms for flood generation on
Earth, Mars, and Titan

Devon Burr
Earth and Planetary Sciences Department
EPS 306
University of Tennessee Knoxville
1412 Circle Dr.
Knoxville TN 39776-1410 USA
dburr1@utk.edu

ABSTRACT

Conditions allow surficial liquid flow on three bodies in the Solar System, Earth, Mars, and Titan. Evidence for surficial liquid *flood* flow has been observed on Earth and Mars. The mechanisms for generating flood flow vary according to the surficial conditions on each body. The most common flood-generating mechanism on Earth is wide-spread glaciation, which requires an atmospheric cycle of a volatile that can assume the solid phase. Volcanism is also a prevalent cause for terrestrial flooding, which other mechanisms producing smaller, though more frequent, floods. On Mars, the mechanism for flood generation has changed over the planet's history. Surface storage of floodwater early in Mars' history gave way to subsurface storage as Mars' climate deteriorated. As on Earth, Mars' flooding is an effect of the ability of the operative volatile to assume the solid phase, although on Mars, this has occurred in the subsurface. According to this paradigm, Titan conditions preclude extreme flooding because the operative volatile, which is methane, cannot assume the solid phase. Mechanisms that produce smaller but more frequent floods on Earth, namely extreme precipitation events, are likely the most important flood generators on Titan.

1. Introduction

The historical flow of paleoflood science has risen and fallen largely in concert with prevailing scientific paradigms (Baker 1998). The paradigm in the 17th century was catastrophism, the idea that geology is the product of sudden, short, violent events. In paleoflood science, this paradigm was expressed as diluvialism, the view that the Biblical flood was historically accurate and could explain various geological formations and fossil remains. Catastrophism gave place to uniformitarianism, first introduced in 1830, which stipulated that the Earth's formations are the product of slow, gradual change. Under this paradigm, geologic formations previously explained by catastrophic (Biblical) flooding were often transmuted into the effects of sustained river flow or of glaciation. The Channeled Scabland, Washington, USA, was originally interpreted as glacial in origin, either directly (through flow of glacial ice) or indirectly (through diversion of rivers). Consequently, the proposal by J. Harlan Bretz of massive flooding as an explanation for the Channeled Scabland was originally treated as an absurd or outrageous hypothesis (cf. Davis 1926, Baker 1978). Decades of study demonstrated the verity of this hypothesis, establishing paleoflood hydrology and geomorphology as a geologic subdiscipline (e.g., Kochel and Baker 1982).

During this time, the study of paleofloods was also extended to Mars. The Mariner 9 and Viking orbiter missions first observed Mars' gigantic flood channels, identified on the basis of their morphologic similarity to the Channeled Scabland (Mars Channel Working Group 1983). Future analysis and follow-on spacecraft missions to Mars supported continued study of these and other flood channels (Baker 1982, Carr 1996), providing quantitative estimates of discharge and other flow parameters, although with large error bars (Wilson et al. 2004). As a result, catastrophic flooding was established as an extraterrestrial pursuit.

The Cassini-Huygens mission to the Saturnian system (Matson et al. 2002) opened up a new frontier in planetary geology. Mission data revealed the surface of Titan, Saturn's largest moon, as having strikingly Earth-like landforms – including aeolian dunes (Lorenz et al. 2006) and lakes (Stofan et al. 2007) –, although comprised of exotically un-Earth-like materials. Fluvial features have been interpreted as river channels (Elachi et al. 2005, Porco et al. 2005, Tomasko et al. 2005), which may have discharges of order $10^4 \text{ m}^3/\text{s}$ (Jaumann et al. 2007). Though much smaller than flood discharges on Mars or Earth, such a discharge would be large for terrestrial rivers.

This paper compares and contrasts evidence for paleofloods on these three planetary bodies, Earth, Mars, and Titan. Each of these three bodies has its own set of conditions and materials (some of which are listed in Table 1), so that each has its own mechanisms for generating floods. This paper compares and contrasts flooding in the Solar System by reviewing the flood morphologies and then the flood generation mechanisms for each of these three bodies in turn.

2. Flooding on Earth

A. Glaciation

The largest paleofloods on Earth, with discharges of order $10^6 - 10^7 \text{ m}^3/\text{s}$, are associated with glaciation (Baker 1996, O'Connor and Costa 2004). The primary mechanism that produced these floods was the sudden release of water from glacial lakes. Proglacial lakes result from damming by the glacier of pre-existing river valleys. These glacial lakes and their outbursts occurred frequently during the Quaternary glaciations as a result of disruption of pre-

existing fluvial drainage (Starkel 1995). Ice-marginal lakes result from impoundment of the glacial meltwater against the glacier margin, commonly by morainal debris. Ice-marginal (or moraine basin) lakes usually store less water than proglacial lakes, and so generally produce relatively smaller discharges (O'Connor and Beebee 2008). The most extensive known examples of glacial lake outburst flooding are located in the northern mid-latitudes, where continental ice sheets disrupted pre-existing fluvial flow (e.g., Grosswald 1998). The most voluminous examples (in terms of discharge) have been found in areas of significant relief where deep valleys supported tall ice dams that impounded large lakes. Earth's largest ice-dam failure floods include: the Kuray and other floods in the Altai Mountains, Siberia, during the Late Pleistocene (Baker et al. 1993; Rudoy 1998; Carling et al. 2002; Herget 2005); the Missoula floods that carved the Channeled Scabland in Washington, USA (Baker 2008 and references therein); and early Holocene floods down the Tsangpo River gorge in southeastern Tibet (Montgomery et al. 2004). The largest ice-marginal or moraine dam failure floods include the Lake Agassiz overflow floods in North America (Kehew et al. 2008 and references therein).

B. Volcanism

In addition to directly producing paleofloods on Earth, glaciation contributes to flood production indirectly in conjunction with near-surface volcanism or enhanced geothermal heat flow (Björnsson 2008). Some of the largest floods associated volcanism result from direct melting of overlying snow and ice by eruption or geothermal heat flow. Persistent subglacial hydrothermal systems may result from the interaction of the resultant glacial meltwater with shallow magmatic intrusions. Continued increase of the subglacial lake volume eventually breaks the hydraulic seal of the overlying glacier, and the meltwater is catastrophically released. This process takes place today in Iceland, as in the 1996 subglacial eruption and resultant jökulhlaup from the Grímsvötn cauldron beneath the Vatnajökull glacier (Figure 1) (Guðmundsson et al. 1997) and the 1918 jökulhlaup from beneath the Kötlujökull glacier (Tómasson 1996). Early Holocene jökulhlaups with discharges of order $10^5 \text{ m}^3/\text{s}$ drained northward from the Kverkfjöll glacier (Carrivick 2005), carving the Jökulsá á Fjöllum flood channel (Waite 2002).

Volcanism also causes flooding by other means than direct melting. Caldera-lake breaching can produce discharges of similar magnitude to ice-dam breaches, as in the case of a late Holocene flood from the Aniakchak volcano, Alaska (Waythomas et al. 1996). More commonly, breaching of water-filled calderas produces floods 1 – 2 orders of magnitude lower. The near instantaneous failure of a large ignimbrite dam at the Lake Taupo, New Zealand, for example, produced a caldera flood of order $10^5 \text{ m}^3/\text{s}$ (Manville et al. 1999). Other examples of large floods from breached volcanoclastic dams include floods from Tarawera caldera, New Zealand (Manville et al. 2007) and the Holocene flood from Mount Mazama, USA (Conaway 1999 in O'Connor and Beebee 2008). Large floods resulted from lava dams on the Colorado River, USA (Fenton et al. 2006), and pyroclastic flows, lahar deposits, and landslides triggered by eruptions have likewise caused flooding.

C. Tectonic Basin Overflow

Volcanic calderas are one of three types of geologic basins that produce flooding, the other two being moraine basins (reviewed in the section on glacial flooding above) and tectonic basins. Floods from tectonic basins can be the volumetrically largest of the three basin-breach

type floods because they can impound the most water (see O'Connor and Costa 2004 and O'Connor and Beebee 2008, from which the following discussion is taken).

Most commonly, floods from closed tectonic basins are a result of the basin becoming filled with water due to sustained positive water balance. This occurred for example during the Quaternary in the basin-and-range province, western USA, where natural tectonic basin filling coincided with glacial advance (Baker 1983, Reheis et al. 2002). Lake Bonneville (Malde 1968, O'Connor 1993) and other Pliocene-Pleistocene lakes in the western USA (see Currey 1990, Reheis et al. 2002) provide examples of tectonic basin-breach floods fed by combined rainfall and groundwater flow.

More rarely, floods may be produced from tectonic basins by sudden input of water. This may have occurred included the lower Colorado River, which may have connected to the upper Colorado drainage about 5 Ma ago due to a series of upstream basin breaches involving large floods (House et al. 2005). And catastrophic breaching of basins may have carved Hells Canyon and the western Snake River gorge, leading to integration with the Columbia River (Othberg 1994; Wood and Clemens 2002).

Earth's geology also records immense marine floods, both into and out of tectonic basins. Flooding of the Mediterranean Basin via a breach at the present-day Straits of Gibraltar (Hsü 1983) is the largest known example of marine flooding. A smaller flood may have occurred when the rising Mediterranean Sea then flooded into the Black Sea via the Bosphorus Strait (Ryan and Pitman 1999).

A common geologic setting for these tectonic basin-breach floods is a semi-arid environment during changing hydrological conditions (O'Connor and Beebee 2008). The negative water balance in semi-arid climates minimizes basin integration, allowing large volumes of water to accumulate over geologic time. The changing hydrological conditions provide the input to eventually trigger the flooding. Freshwater floods are associated with pluvial periods during glacial advance, and marine floods probably resulted from sea level rise during deglaciation.

D. Other natural dam failures: landslides and ice-jams

Two other times of dam breaches cause catastrophic flooding. Landslides that were not directly related either to glacial or volcanic conditions caused two of Earth's 27 largest floods (O'Connor and Costa 2004). Landslide dams can form in a wide variety of settings, and are most commonly triggered by lubrication due to water (precipitation or snowmelt) or by earthquakes. As with glacial ice or moraine dams, the potential discharge increases with increasing dam height (O'Connor and Beebee 2008).

Ice-jam floods account for three of Earth's largest known floods (O'Connor and Costa 2004), all of which occurred on the Lena River, Russia (Rodier and Roche 1984). Ice jam flooding occurs when broken river ice accumulates at constrictions or bends in the river, causing ponding upstream of the constriction and sudden release when the ice jam breaks. Large, northward-flooding arctic rivers are thus most susceptible to ice-jam flooding because the southern reaches are more likely to thaw and flow before the northern reaches.

E. Precipitation

Precipitation-fed floods, along with ice-jam floods, are Earth's smallest floods. These 'meteorological floods' (O'Connor and Costa 2004) result from extreme precipitation events, e.g., monsoons. Thus, the largest such floods occur in tropical climates dominated by monsoons

or tropical storms. Flood size is also correlated with river basin size, because the largest river basins receive the largest total amount of rain. The Amazon River in South American, which drains the world's largest basin with an area of 7 million km², has produced 3 of the four precipitation-fed floods, and the Yangtze River of China has produced the fourth.

In summary, Earth's largest flood result from glaciation, with smaller discharge floods contributed by volcanism in conjunction with glaciation, and much smaller floods from ice-jams on polar rivers. Thus, for these mechanisms, the planetary body needs a volatile that is close to the freezing point. Tectonism in semi-arid climates produces significant basin-breach floods.

3. Flooding on Mars

The causes for flooding on Mars are less well known than for flooding on Earth because *in situ* data are not yet available from Martian flood channels and because Martian flooding has not been observed. Thus, unlike for Earth, flooding on Mars cannot be analyzed solely on the basis of flood-producing mechanisms. However, Martian channels have distinctive morphologies that may be grouped into three categories which roughly correspond with Mars' three chronostratigraphic epochs. On the basis of these morphologies, flood mechanisms can be discussed.

A. Noachian flooding from large basins

Mars' oldest channels date to the late Noachian epoch (>3.7 Ga; dates of Martian epochs are based on Tanaka 1986 and Hartmann and Neukum 2001), a time of inferred warmer and wetter climate than at present (Carr 1996). These channels originate at large basins formed either by impact cratering or by intercrater plains topography (Irwin and Grant 2008). Several such basin overflow channels have been inferred for Mars (see Irwin and Grant 2008, Table 1), of which the three most distinct are discussed here.

Mars' longest basin overflow channel is the segmented meso-outflow Uzboi-Ladon-Margaritifer (ULM) channel system (Saunders 1979, Baker 1982). The ULM channel originates full width at the northern edge of the large Argyre impact crater basin, from which it stretches several hundred kilometers northward to the Margaritifer topographic basin. Argyre itself was fed through several other large valley systems (Parker 1985, 1994), so that the total contributing area to the ULM system was $\sim 10^7$ km², or about 9% of Mars (Banerdt 2000, Phillips et al. 2001). Subsequent cratering of proximal ULM has obscured immediate outlet area, and thus the water release mechanism. However, deeply incised reaches, nearly constant widths, hanging valleys, small streamlined forms, and a poorly developed tributary network all suggest formation by flooding (Irwin and Grant 2008). Discharge estimates vary from 150,000 m³/s to 450,000 m³/s (see Irwin and Grant 2008 and references therein).

Ma'adim Vallis, like the ULM system, has a wide, deep main channel and originates full width at the northern side of an enclosed basin. This source basin is a product of intercrater plains topography, with multiple sub-basins, and covers $\sim 10^6$ km² (Irwin et al. 2002, 2004). Flooding in Ma'adim Vallis is suggested by the channel's nearly constant width, adjacent hanging valleys, and longitudinal ridges on the channel floor. The calculated discharge is consistent with a dam breach of ~ 100 m depth, which is less than half of the total observed breach depth. And adequate water could have been stored in the present-day source basin to carve Ma'adim Vallis with reasonable water:sediment ratios (see Irwin and Grant 2008 and references therein).

Mawrth Valles is the smallest of these late Noachian flood channels, and appear to have originated at the Margaritifer basin, an intercrater basin which would have received discharge from the ULM channel system (Irwin and Grant 2008). This is based on reconstruction, however, as overflow from Margaritifer at Mawrth's origination point is not possible with current topography. That is, flow would first spill over at lower points to the east. Possible explanations include tilting due to growth of the nearby Tharsis volcanic edifice and/or the influx of ULM floodwaters as discussed above (Irwin and Grant 2008).

B. Hesperian flooding from chaos and chasmata

Mars' largest flood channels are enormous in size, with widths up to several tens of kilometers, lengths of hundreds of kilometers, and depths of over a thousand meters (Figure 2) (Smith et al. 1998). These channels debouch into Chryse Planitia, located northeast of the Valles Marineris canyon system, and are collectively referred to as the circum-Chryse channels. Smaller Hesperian-aged channels are also found at the eastern end of Valles Marineris, south of Chryse Planitia. All these channels date to the Hesperian epoch (3.7 – 3.0 Ga), an era of declining surface conditions from a warm, wet climate to cold, dry conditions.

These Hesperian-aged channels may be grouped according to their size and morphology at origin (Coleman and Baker 2008). The largest, circum-Chryse channels generally originate at chasmata. Chasmata are deep, steep-sided depressions, which commonly contain chaos, areas of kilometer-sized or larger blocks surrounded by flatter, lower elevation terrain (Figure 2) (see <http://planetarynames.wr.usgs.gov/jsp/append5.jsp> for definitions of descriptor terms).

Chasmata and their inset chaos are attributed to surface collapse as a result of subsurface volatile (water) outburst (e.g., Carr 1996 and references therein, Rodriguez et al. 2006). The cause of the outbursting likely involved pressurization of groundwater by a growing cryosphere (Clifford and Parker 2001). Cryosphere disruption could have been caused by magmatic intrusions (Leask et al. 2006), cryosphere melting (McKenzie and Nimmo 1999), and/or by dissociation of CO₂ ice or clathrate (Komatsu et al. 2000). In the few instances of chaos on channel floors, outbursting may have been triggered by flood erosion that reduced the overburden pressure (Coleman 2005).

Following outbreak of water from a pressurized aquifer, lakes apparently formed in these chasmata and then overflowed, as indicated by topographic relationships among inferred spillways, scabland, or other flood-formed features (see Coleman and Baker 2008 and references therein). The interpretation of layered deposits within the chasmata as lacustrine sediments (Lucchitta et al. 1992) was an early indication of this possibility. The overflow flooding may have been triggered by failure of debris- or ice-barriers between chasmata, resulting in sudden influxes of water from other chasmata-lakes (Coleman and Baker 2008). However, other suggested mechanisms for flooding, such as catastrophic release from extensive caverns (Rodriguez et al. 2005), do not require surface storage of water.

Although smaller, the Hesperian-aged channels east of Valles Marineris may have had a similar flood generating mechanism. These channels lack chasmata at their origins and so are unlikely to have had lakes or other surface water sources. However, various surface features suggest lateral subsurface flow ways from a distal chasmata to channel origins, perhaps augmented by ground ice melting (Carr 1995, Cabrol et al. 1997, Rodriguez et al. 2003). The relative elevations of these channels in comparison to the massive Tharsis volcanic edifice would have allowed magmatic recycling of groundwater (cf. Gulick 1998) to have fed these inferred paleolakes (Coleman et al. 2007).

Thus, the source for Mars' Hesperian-aged flood channels was a mixture of ponded surface water and pressurized subsurface water. The contribution from both these sources may have given rise to these largest of Martian floods.

C. Amazonian flooding from extensional fossae

Four of Mars' flood channels dated to the Amazonian epoch (3.0 Ga to present), with model ages ranging from earliest Amazonian to the last few Ma. Width and depth dimensions roughly an order of magnitude smaller than those of Mars' Hesperian-aged, circum-Chryse channels (Burr et al. 2008).

These channels originate at fossae (e.g, Figure 3), defined as long, narrow depressions (see <http://planetarynames.wr.usgs.gov/jsp/append5.jsp>). The fossae have varied morphologies, suggesting multiple possible mechanisms for floodwater release. Some of the fossae have graben morphology, which is interpreted to reflect subsurface dikes (Wilson and Head 2002, Head et al. 2003, Ghatan et al. 2005, Leask et al. 2007). In these cases, the floodwater release mechanism is inferred to have been cracking by the dike of a confining cryosphere and release of pressurized groundwater. The westward migration through time of both volcanic and aqueous flooding from the Cerberus Fossae is consistent with a volcanic triggering mechanism (see Burr et al. 2008 and references therein).

Alternatively or additionally, fossae may be the result amagmatic extensional tectonics. Based on inferred hydrologic properties of the Martian crust (Hanna and Phillips 2005), modeling shows that extensional stress relief can produce sufficient excess pore pressures to drive catastrophic release of groundwater (Hanna and Phillips 2005). This mechanism may have acted in concert with other factors, such as increased elevational head in the form of perched aquifers (cf. Tanaka and Chapman 1990) or aquifer pressurization due to cryosphere growth (Clifford and Parker 2001), but does not require them.

Ice-rich ground may have been melted (Zimbelman et al. 1992), perhaps by the dike intrusion (cf. Head et al. 2003), providing water and sediment contribution to the flood discharge. However, melting by dike intrusion alone is not sufficient to release floodwater at the volumetric rate modeled from surface channel size and slope (cf. McKenzie and Nimmo 1999), which is of order 10^5 - 10^6 m³/s for channels that head at fossae (see discussion and references in Burr et al. 2008). Short-term ponding may have occurred in the fossae before breaching and/or overflowing the fossae rim (Ghatan et al. 2005, Keszthelyi et al. 2007), contributing to high instantaneous discharges.

Given the variety of fossae morphology at the outflow channels' origins, it is likely that multiple floodwater mechanisms gave rise to Mars' most recent floods.

In summary, Mars' Noachian floods generated by overflow from impact crater or intercrater topographic basins. These floods were the lowest in discharge and apparently the fewest in number, although continual improvements in data may modify that perception (e.g., Mangold et al. in revision). Flooding during the Hesperian was the most voluminous and likely involved both surface and sub-surface water sources, which likely explains the maximal discharge during this time. Amazonian-aged flooding from fossae was fed by subsurface sources. Megaflooding on Mars may be summarized visually with Figure 4.

For comparison between the two planets, Mars' Noachian basin overflow flooding, as well as putative chasmata-lake overflows, is similar to basin-breach flooding on Earth. As on Earth, this requires a climate that generates precipitation. Hypothesized mechanisms that invoke

a pressurized aquifer are dissimilar to any terrestrial mechanisms. However, triggering due to volcano-ice interactions is similar in concept to terrestrial floods produced by volcanic events, although different in context (i.e., subsurface versus surface).

4. Flooding on Titan?

Flooding on Titan occurs with very different materials and conditions than on Earth and Mars. Flooding on Earth and Mars entails water flow and the sediment is silicate material. However, models of Titan relegate any silicate material to its core (Tobie et al. 2006). Water on Titan is in the solid phase and largely comprises Titan's crust (Griffith et al. 2003, Lorenz and Lunine 2005). Thus, given sufficient erosion on Titan (Lorenz and Lunine 1996), fluvial sediment is likely composed of water ice grains. An alternative or additional source of fluvial sediment is organic material derived from the atmosphere through photochemical reactions of hydrocarbons (Waite et al. 2007 and references therein). At Titan's surface temperature (~94K) and pressure (~1.44 bar), liquid flow would entail hydrocarbons, likely a mixture of methane and nitrogen (Lorenz et al. 2003, Lorenz and Lunine 2005). Despite these differences between materials on Titan, Earth, and Mars, however, theoretical modeling using the values in Table 1 shows that sediment transport parameters are similar on the three bodies (Burr et al. 2006). Fluvial erosional processes may also to be similar (Collins 2005).

Images from multiple instruments both on the Cassini spacecraft (Porco et al. 2005, Elachi et al. 2005, Tomasko et al. 2005, Barnes et al. 2007) and on the Huygens probe (Tomasko et al. 2005) show elongate, sinuous features inferred to be fluvial channels (Figure 5), although they may more likely be fluvial valleys (Perron et al. 2006, Burr 2007). Some of these features are a few hundred meters in width, and an empirical relationship between discharge and width scaled for Titan gravity suggests that these features, if true channels, may have transported of order $10^3 \text{ m}^3/\text{s}$ of material (Jaumann et al. 2007), similar to large river systems on Earth.

Of interest here is whether these fluvial channels on Titan show evidence for paleoflooding. Some of these features have an anastomosing appearance in plan view, similar to that of terrestrial desert flood channels produced by monsoonal rains (Lorenz et al. 2008). Titan is hypothesized to have a 'methane monsoon' (Lorenz and Mitton 2002) on the basis of theory and observations (Lorenz et al. 2005). However, at present, rain is apparently falling slowly and continuously on Titan (Tokano et al. 2006, Ádámkovics et al. 2007). Thus, if the anastomosing features are indeed flood channels, they may indicate a previous epoch of different climatic conditions (Lunine and Atreya 2008).

A glacial flood mechanism is unlikely on Titan, given the triple point of hydrocarbon (see Lorenz and Lunine 2005). However, images and spectra indicate the occurrence of cryovolcanism on Titan (Sotin et al. 2005, Lopes et al. 2007). By analogy with volcanism on Earth, Titan's cryovolcanism may provide the geologic context for debris-dam floods; calderas large enough to generate floods have not yet been inferred from Cassini-Huygens data published to date, but may be also possible. The impact crater population on Titan is sparse (Lorenz et al. 2007a), but examples of possible impact craters show elongate sinuous features on their flanks. These features may be either lava channels or fluvial channels (Lopes et al. 2007). If fluvial channels, they may indicate floods from craters analogous in mechanism to basin-breach floods that occur from overflow of martian impact crater basins. Titan topography is muted relative to Earth or Mars (Lorenz et al. 2007b), so topographic basin-breach flooding may be less likely.

A comparison of flooding on Earth, Mars, and Titan is summarized in Table 2. The largest floods on Earth and on Mars are produced in an atmospheric volatile cycle in which the volatile can easily assume the solid phase. On Earth, this solid phase is a surficial phenomenon, whereas on Mars it is apparently a subsurface phenomenon. On Titan, the temperature and pressure conditions render such catastrophic paleofloods unlikely because the volatile is unlikely to assume the solid phase. However, the least important mechanism for generating floods on Earth and Noachian-age Mars, namely precipitation, is likely the most important flood generating mechanism on Titan. Whereas on Earth and Mars, this mechanism generated basin-overflow floods, on Titan, heavy precipitation appears more likely to (have) cause(d) floods directly.

Catastrophic flooding changed the climate on Earth and Mars. Continued investigations may indicate if or how flooding changed the climate on Titan.

TABLE 1: Some parameters of interest for Earth, Mars, and Titan.

Parameter	Earth	Mars	Titan
Surface gravity (m/s^2)	9.81	3.71	1.35
Surface temperature (K)	287	210	94
Surface pressure (bars)	1.01	0.007	1.44
Fluvial liquid, density (kg/m^3), viscosity (Pa s)	Water, 1000, 1×10^{-3} Pa s	Water, 1000, 1×10^{-3} Pa s	CH_4/N_2 , 450, 2×10^{-4} Pa s
Fluvial sediment, density (kg/m^3)	Quartz, 2650	Basalt, 2900	Water ice, 992 Organics, 1500
Atmospheric composition	$\sim 79\% \text{ N}_2$, $20\% \text{ O}_2$	$\sim 95\% \text{ CO}_2$, $2.7\% \text{ N}_2$	$\sim 95\% \text{ N}_2$, $\sim 5\% \text{ CH}_4$

Titan fluid density and viscosity values from Lorenz et al. (2003); organic density from Khare et al. (1994), but lower values are possible.

Table 2: summary of comparison among flood generating mechanisms on Earth, Mars, and Titan.

<u>Cause:</u>	Earth	Mars	Titan
glaciation	most significant direct cause	possible, but evidence not observed	unlikely, given materials, surface conditions on Titan
volcanism/ geothermal heat flow	significant direct cause, most important indirect cause	Hesperian chaos terrain floods, Amazonian fissure floods (alternative=tectonism)	possible, since evidence for cryovolcanism observed
dam-failure	important indirect cause (post-glaciation); ice jams	Noachian basin overflow floods, Hesperian chasmata floods	dams of cryovolc. material possible; morainal dams unlikely
precipitation	monsoon important in tropics, snowmelt in continental inlands	Noachian basin overflow floods	‘methane monsoon’ most significant cause on Titan?

FIGURES

Figure 1: Oblique aerial photo of 1996 jökulhlaup at Skeiðarársandur, Iceland, Nov 1996. Flow from Vatnajökull glacier is toward the viewer; two-lane bridge in photo center suggests scale. (Photo by Magnus Tumi Guðmundsson and Finnur Paulson)



Figure 2: Topography showing the western-most circum-Chryse channels. Black box shows location of black-and-white mosaic; annotated length of Valles Marineris suggests scale. Black-and-white image is a mosaic of day infrared images showing an example of chaos terrain located in Eos Chasma (image center; chaos also visible to the right and lower left). (Topography credit: MOLA team. Mosaic credit: THEMIS team/ASU.)

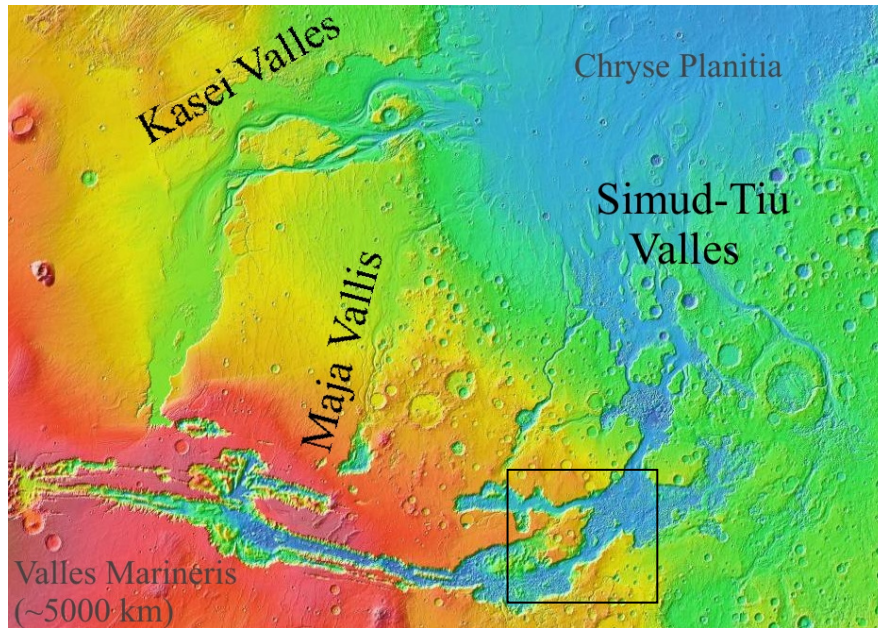


Figure 3: Topography of Mangala Valles. Channel originates at the notch in the northern side of the fissure (below lowest arrow) and stretches northward (note streamlined form in image center below middle black arrow), before diverging into two channels. Channel is ~550 km long from fossae to divergence.

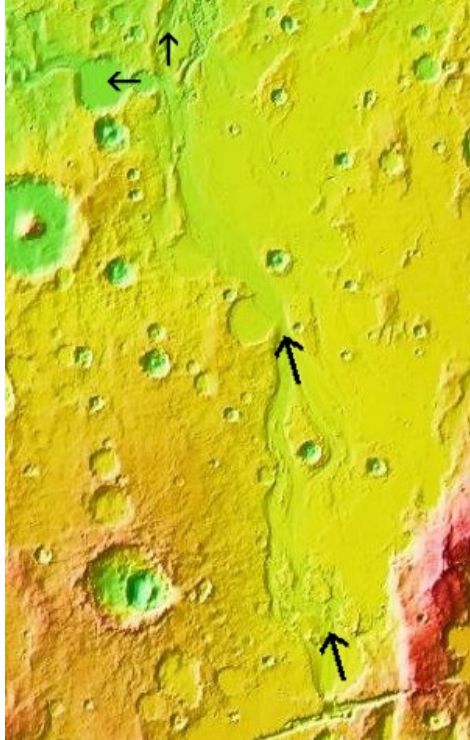


Figure 4: Schematic plot showing relative frequency of flooding through Mars' history.

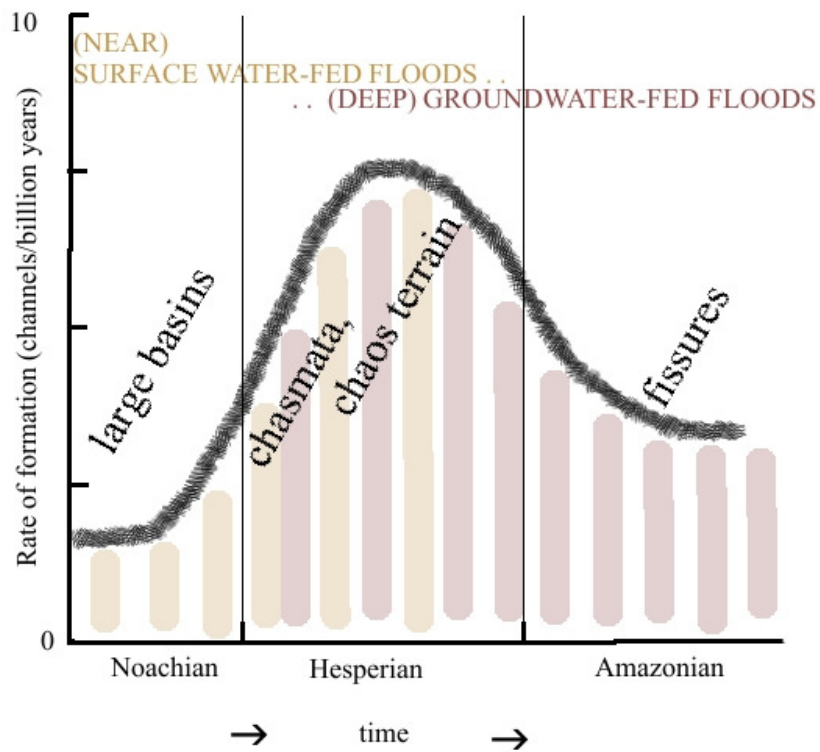
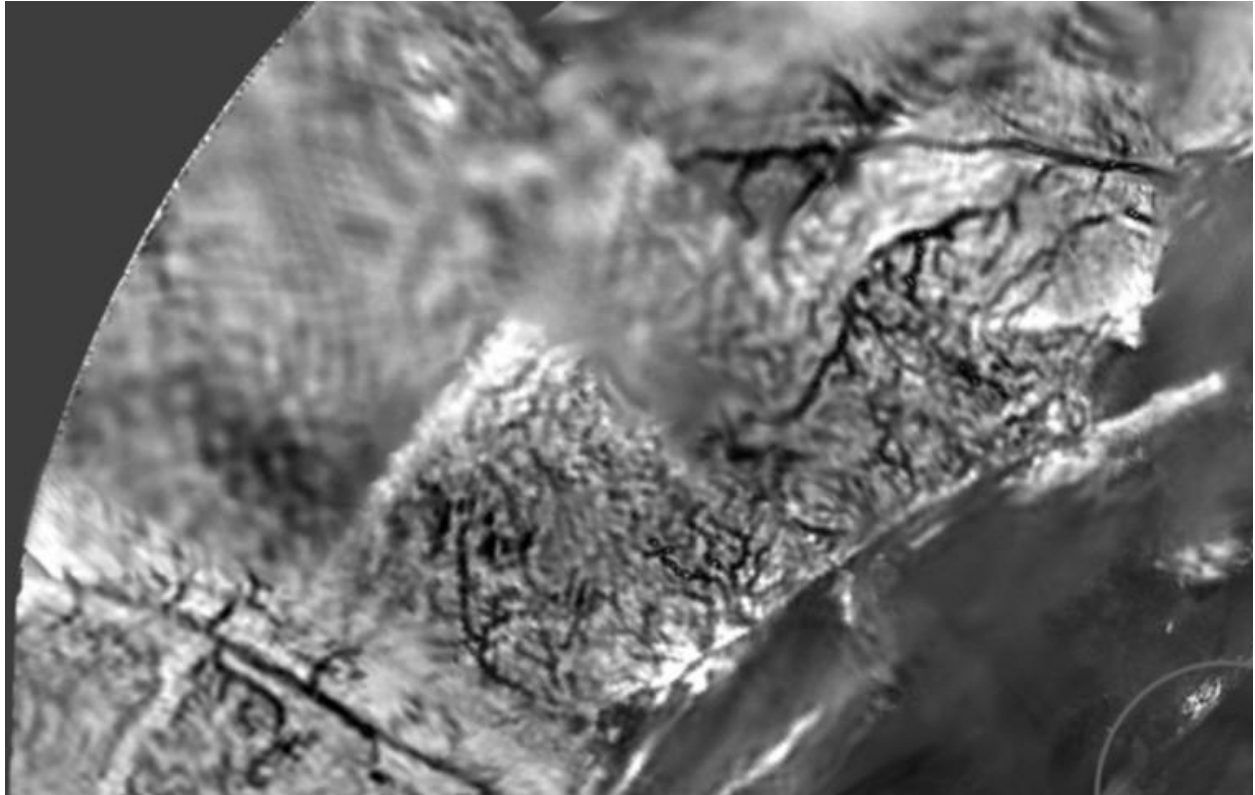


Figure 5: Image mosaic from the Descent Imager/Spectral Radiometer on the Huygens probe, showing inferred fluvial channels and a dry lake bed shoreline. The image is ~12 km wide. The arc in the lower right is an artificial marking. (Image Credit: ESA/NASA/JPL/University of Arizona).



REFERENCES

- Ádámkovics, M., Wong, M.H., Laver, C., de Pater, I., 2007. Widespread morning drizzle on Titan. *Science* 318, 962-965,
- Baker, V.R., 1978. The Spokane Flood Controversy. In: Baker, V.R., Nummedal, D. (Eds.), *The Channeled Scabland*. NASA, Washington, D.C., pp. 3-15.
- Baker, V.R., 1982. *The Channels of Mars*. Austin: University of Texas Press.
- Baker, V.R., 1983. Late Pleistocene fluvial systems. In *The Late Pleistocene*, ed. S.C. Porter, Volume 1 of *Late-Quaternary Environments of the United States*, ed. H.E. Wright, Jr., Minneapolis, MN: University of Minnesota Press, pp. 115-129.
- Baker, V.R., 1996. Megafloods and glaciation. In: Martini, I.P. (Ed.), *Late Glacial and Postglacial Environmental Changes*. Oxford University Press, pp. 98-108.
- Baker, V.R., 1998. Catastrophism and uniformitarianism: logical roots and current relevance. In: Blundell, D.J., Scott, A.C. (Eds.), *Lyell: the Past is the Key to the Present*. Geological Society of London, Spec. Publication 143, Geological Society of London, Bath, pp. 171-182.
- Baker, V.R., 2008. Channeled Scabland morphology. In: Burr, D.M., Baker, V.R., Carling, P.A. (Eds.), *Megaflooding on Earth and Mars*. Cambridge University Press.
- Baker, V.R., Benito, G., Rudoy, A.N., 1993. Paleohydrology of Late Pleistocene superflooding, Altay Mountains, Siberia. *Science*, **259**, 348-350.
- Barnes, J.W., Radebaugh, J., Brown, R.H., Wall, S., Soderblom, L., Lunine, J., Burr, D., Sotin, C., Le Mouélic, S., Rodriguez, S., Buratti, B.J., Clark, R., Baines, K.H., Jaumann, R., Nicholson, P.D., Kirk, R.L., Lopes, R., Lorenz, R.D., Mitchell, K., Wood, C.A., 2007. Near-infrared spectral mapping of Titan's mountains and channels. *J. Geophys. Res.* 112, E11006, 10.1029/2007JE002932.
- Björnsson, H., 2008. Jökulhlaups in Iceland: sources, release and drainage. In: Burr, D.M., Baker, V.R., Carling, P.A. (Eds.), *Megaflooding on Earth and Mars*. Cambridge University Press.
- Burr, D.M., 2007. Fluvial flow on Titan: context for geomorphic interpretation. *Outer Solar System Satellites Workshop*, Boulder, CO, Aug 13-15 (Abstract 6088).
- Burr, D.M., Emery, J.P., Lorenz, R.D., Collins, G.C., Carling, P.A., 2006. Sediment transport by liquid overland flow: application to Titan. *Icarus* **181**, 235-242, doi:10.1016/j.icarus.2005.11.012
- Burr, D.M., Wilson, L., Bargery, A.S., 2008. Floods from fossae: a review of Amazonian-aged extensional-tectonic megaflood channels on Mars. In: Burr, D.M., Baker, V.R., Carling, P.A. (Eds.), *Megaflooding on Earth and Mars*. Cambridge University Press.

Cabrol, N. A., Grin, E. A., Dawidowicz, G., 1997. A model of outflow generation by hydrothermal underpressure drainage in volcano-tectonic environment, Shalbatana Vallis (Mars). *Icarus*, **125**, 455-464.

Carling, P.A., Kirkbride, A.D., Parnachov, S., Borodavko, P.S., Berger, G.W., 2002. Late Quaternary catastrophic flooding in the Altain Mountains of south-central Siberia: a synoptic overview and an introduction to flood deposit sedimentology. In: Martini, I.P., Baker, V.R., and Garzón, G. (Eds.), *Flood and Megaflood Processes and Deposits: Recent and Ancient Examples*. Spec. Publs int Ass. Sediment. 32, pp. 17-35.

Carr, M.H. 1996. *Water on Mars*. Oxford University Press, New York.

Carrivick, J.L., 2005. Characteristics and impacts of jökulhlaups (glacial outburst floods) from Kverkfjöll, Iceland. Keele University unpublished PhD thesis.

Coleman, N. M., Dinwiddie, C. L., Casteel, K., 2007. High outflow channels on Mars indicate Hesperian recharge at low latitudes. *Icarus*, **189**, doi:10.1016/j.icarus.2007.01.020, 344–361.

Coleman, N.M., Baker, V.R., 2008. Surface morphology and origin of outflow channels in the Valles Marineris region. In: Burr, D.M., Baker, V.R., Carling, P.A. (Eds), *Megaflooding on Earth and Mars*. Cambridge University Press.

Collins, G.C., 2005. Relative rates of fluvial bedrock incision on Titan and Earth. *Geophys. Res. Lett.* **32**, L22202, doi:10.1029/2005GL024551.

Conaway, J.S., 1999. Hydrogeology and paleohydrology of the Williamson River basin, Klamath County, Oregon. Unpublished M.S. thesis, Portland State University, Portland, Oregon.

Currey, D.R., 1990. Quaternary palaeolakes in the evolution of semidesert basins, with special emphasis on Lake Bonneville and the Great Basin, U.S.A. *Palaeogeography, Palaeoclimatology, and Palaeoecology*, **76**, 189-214.

Davis, W.M., 1926. The value of outrageous geological hypotheses. *Science* **63**, no. 1636, 463-468.

Elachi. C. and 34 co-authors, 2005. Cassini Radar Views the Surface of Titan. *Science* **308**, 970-974.

Fenton, C.R., Webb, R.H., Cerling, T.E., 2006. Peak discharge of a Pleistocene lava-dam outburst flood in Grand Canyon, Arizona, USA. *Quaternary Research*, **65** (2). 324-335.

Ghatan, G.J., Head, J.W., Wilson, L., 2005. Mangala Valles, Mars: assessment of early stages of flooding and downstream flood evolution. *Earth Moon Planets*, **96**, (1-2), 1-57, doi: 10.1007/s11038-005-9009-y.

Griffith, C.A., Owen, T., Geballe, T.R., Rayner, J., Rannou, P., 2003. Evidence for exposure of water ice on Titan's surface. *Science* 300, 628–630.

Grosswald, M.G., 1998. New approach to the ice age paleohydrology of northern Eurasia. In: Benito, G., Baker, V.R., Gregory, K.J. (Eds.), *Palaeohydrology and Environmental Change*, Wiley, Chichester, pp. 199-214.

Gulick, V.C., 1998. Magmatic intrusions and a hydrothermal origin for fluvial valleys on Mars. *J. Geophys. Res.* 103, 19,365–19,387.

Guðmundsson, M T., Sigmundsson, F., Björnsson, H. 1997. Ice-volcano interaction of the 1996 Gjalp subglacial eruption, Vatnajökull, Iceland. *Nature*, **389**, 954-957.

Hartmann, W. K., G. Neukum, 2001. Cratering chronology and evolution of Mars. In *Chronology and Evolution of Mars*, (eds., R. Kallenbach, J. Geiss, W. K. Hartmann), Space Sci. Rev., 96, 165– 194.

Hanna, J.C., Phillips, R.J., 2005. Hydrological modeling of the Martian crust with application to the pressurization of aquifers, *J. Geophys. Res.*, 110, E01004, doi: 10.1029/2004JE002330.

Hanna, J.C., Phillips, R.J., 2006. Tectonic pressurization of aquifers in the formation of Mangala and Athabasca Valles, Mars, *J. Geophys. Res.*, 111, E03003, doi:10.1029/2005JE002546.

Head, J.W. III, Wilson, L., Mitchell, K.L., 2003. Generation of recent massive water floods at Cerberus Fossae, Mars by dike emplacement, cryospheric cracking, and confined aquifer groundwater release. *Geophys. Res. Lett.* 30(11), 1577, doi:10.1029/2003GL0117135.

Herget, J., 2005. Reconstruction of Pleistocene ice-dammed lake outburst floods in the Altai Mountains, Siberia. *Geological Society of America Special Paper 386*. Geological Society of America.

House, P.K., Pearthree, P.A., Howard, K.A., Bell, J.W., Perkins, M.E., Faulds, J.E., Brock, A.L., 2005. Birth of the lower Colorado River—Stratigraphic and geomorphic evidence for its inception near the conjunction of Nevada, Arizona, and California. In *Interior Western United States: Geological Society of America Field Guide 6*, ed. J. Pederson and C.M. Dehler. Geological Society of America, pp. 358-387.

Irwin, R.P., III, Maxwell, T.A., Howard, A.D., Craddock, R.A., Leverington, D.W., 2002. A large paleolake basin at the head of Ma'adim Vallis, Mars, *Science*, 296, 2209–2212.

Irwin, R.P., III, Howard, A.D., Maxwell, T.A., 2004. Geomorphology of Ma'adim Vallis, Mars, and associated paleolake basins, *J. Geophys. Res.*, 109, E12009, doi:10.1029/2004JE002287.

Irwin, R.P. III, Grant, J.A., 2008. Large basin overflow floods on Mars. In: Burr, D.M., Baker, V.R., Carling, P.A. (Eds), *Megaflooding on Earth and Mars*. Cambridge University Press.

Jaumann, R., Brown, R.H., Stephan, K., Soderblom, L.A., Sotin, C., Le Mouélic, S., Rodriguez, S., Clark, R.N., Barnes, J., Buratti, B.J., McCord, T.B., Baines, K.H., Cruikshank, D.P., Griffith, C.A., Nicholson, P.D., Wagner, R., 2007. Surface erosion of Titan. *Lunar Planet Sci.* XXXVIII (abstract 2100).

Keszthelyi, L., Denlinger, R.P., O'Connell, D.R.H., Burr, D.M., 2007. Initial insights from 2.5D hydraulic modeling of floods in Athabasca Valles, Mars. *Geophys. Res. Lett.* 34, L21206, doi:10.1029/2007GL031776.

Kochel, R.C., Baker, V.R., 1982. Paleoflood hydrology. *Science* 215, no.4531, 353-361.

Komatsu G, Kargel J., Baker V., Strom R., Ori G., Mosangini C., Tanaka K., 2000. A chaotic terrain formation hypothesis: explosive outgas and outflow by dissociation of clathrate on Mars. *Lunar and Planetary Science Conference* [CD-ROM], XXXI, Abstract 1434.

Leask, H.J., Wilson, L., Mitchell, K.L., 2006. Formation of Aromatum Chaos, Mars: Morphological development as a result of volcano-ice interactions. *J. Geophys. Res.* 111, E08071.

Lopes, R.M. and 43 co-authors, 2007. Cryovolcanic features on Titan's surface as revealed by the Cassini Titan Radar Mapper. *Icarus* 186, 395-412, doi:10.1016/j.icarus.2006.09.006.

Lorenz, R.D., Lunine, J.I., 1996. Erosion on Titan: Past and present. *Icarus* 122, 79-91.

Lorenz, R.D., Mitton, J., 2002. Lifting Titan's Veil. Cambridge University Press, 260 pp.

Lorenz, R.D., Lunine, J.I., 2005. Titan's surface before Cassini. *Planet. Space Sci.* 53, 557-576.

Lorenz, R.D., Kraal, E., Asphaug, E., Thomson, R.E., 2003. The seas of Titan. *Eos* 84 (14), 125, 131-132.

Lorenz, R.D., Griffith, C.A., Lunine, J.I., McKay, C.P., Renno, N.O., 2005. Convective plumes and the scarcity of Titan's clouds. *Geophys. Res. Lett.* 32, L01201.

Lorenz, R.D. and 39 co-authors, 2006. The Sand Seas of Titan: Cassini RADAR Observations of Longitudinal Dunes. *Science* 312, 5774, 724-727.

Lorenz, R. D., Wood, C. A., Lunine, J. I., Wall, S. D., Lopes, R. M., Mitchell, K. L., Paganelli, F., Anderson, Y. Z., Wye, L., Tsai, C., Zebker, H., Stofan, E. R., 2007a. Titan's young surface: Initial impact crater survey by Cassini RADAR and model comparison. *Geophys. Res. Lett.* Volume 34, Issue 7, CiteID L07204, doi: 10.1029/2006GL028971.

Lorenz, R.D. and 16 co-authors, 2007b. Titan's shape, radius, and landscape from Cassini Radar altimetry. *Lunar Planet. Sci.* XXXVIII, abstract 1329.

Lorenz, R.D. and 13 co-authors, 2008. Fluvial channels on Titan: initial Cassini Radar observations. *Planet. Space Sci.* in revision.

Lucchitta, B. K., McEwen, A. S., Clow, G. D., Geissler, P. E., Singer, R. B., Schultz, R. A., Squyres, S. W., 1992. The canyon system on Mars. In *Mars* (Kieffer, H. H., et al., eds) University of Arizona Press, Tucson, pp. 453-492.

Lunine and
Malde, H.E. (1968). The catastrophic late Pleistocene Bonneville Flood in the Snake River Plain, Idaho, U.S. Geological Survey Professional Paper 596. U.S. Geological Survey.

Manville, V., White, J.D.L., Houghton, B.F., Wilson, C.J.N., 1999. Paleohydrology and sedimentology of a post-1.8 km breakout flood from intracaldera Lake Taupo, North Island, New Zealand. *Geol. Soc. Am. Bull.* 111(10), 1435-1447.

Manville, V., Hodgson, K.A., Nairn, I.A., 2007. A review of break-out floods from volcanogenic lakes in New Zealand. *New Zealand Journal of Geology & Geophysics*, 50, 131 - 150.

Mars Channel Working Group, 1983. Channels and valleys on Mars. *Geol. Soc. Am. Bull.* 94, 1035-1054.

Matson, D.L., Spilker, L.J., Lebreton, L.J., 2002. The Cassini-Huygens mission to the saturnian system. *Space Sci. Rev.* 104, 1-58.

McKenzie, D., Nimmo, F., 1999. The generation of martian floods by the melting of ground ice above dykes. *Nature* 397 (6716), 231-233.

Montgomery, D.R., Hallet, B., Yuping, L., Finnegan, N., Anders, A., Gillespie, A., Greenberg, H.M., 2004. Evidence for Holocene megafloods down the Tsangpo River gorge, southeastern Tibet. *Quaternary Research* 62, 201-207.

O'Connor, J.E., 1993. Hydrology, hydraulics, and geomorphology of the Bonneville Flood. *Geological Society of America Special Paper 274*. Geological Society of America.

O'Connor, J.E., Costa, J.E., 2004. The world's largest floods, past and present – Their causes and magnitudes. U.S. Geological Survey Circular 1254, 13 p.

O'Connor, J.E., Beebe, R.A., 2008. Floods from natural rock-material dams. In: *Megaflooding on Earth and Mars*, D.M. Burr, V.R. Baker and P.A. Carling, eds. Cambridge University Press.

Othberg, K.L., 1994. *Geology and Geomorphology of the Boise Valley and Adjoining Areas, Western Snake River Plain, Idaho. Bulletin 29, Idaho Geological Survey.*
Moscow, ID: Idaho Geological Survey Press.

Perron, J.T., Lamb, M.P., Koven, C.D., Fung, I.Y., Yager, E., Adamkovics, M., 2006. Valley formation and methane precipitation rates on Titan, *J. Geophys. Res.*, 111, E11001, doi:10.1029/2005JE02602.

Phillips, R.J., Zuber, M.T., Solomon, S.C., Golombek, M.P., Jakosky, B.M., Banerdt, W.B., Williams, R.M.E., Hynek, B.M., Aharonson, O., Hauck II, S.A., 2001. Ancient geodynamics and global-scale hydrology on Mars. *Science*, 291, 2587–2591.

Porco, C.C. and 25 co-authors. 2005. Imaging of Titan from the Cassini spacecraft. *Nature* **434**, 159-168.

Reheis, M.C. Sarna-Wojcicki, A.M., Reynolds, R.L., Repenning, C.A. and Mifflin, M.D., 2002. Pliocene to Middle Pleistocene lakes in the western Great Basin: ages and connections. In *Great Basin Aquatic Systems History*, ed. R. Hershler, D.B. Madsen and D.R. Currey. Washington D.C.: Smithsonian Institution Press, pp. 53-108.

Rodier, J.A., Roche, M., 1984. World catalogue of maximum observed floods. *International Association of Hydrologic Sciences Publication* 143, 354 p.

Rodriguez, J. A., Sasaki, S., Miyamoto, H., (2003). Nature and hydrological relevance of the Shalbatana complex underground cavernous system. *Geophysical Research Letters*, **30**, 1304, doi:10.1029/2002GL016547.

Rodriguez, J. A., Sasaki, S., Kuzmin, R. O., Dohm, J. M., Tanaka, K. L., Miyamoto, H., Kurita, K., Komatsu, G., Fairén, A. G., and Ferris, J. C., 2005. Outflow channel sources, reactivation, and chaos formation, Xanthe Terra, Mars. *Icarus*, **175**, 36-57.

Rodriguez, J. A. P., Kargel, J., Crown, D.A., Bleamaster, L.F., III, Tanaka, K.L., Baker, V., Miyamoto, H., Dohm, J.M., Sasaki, S., Komatsu, G., 2006. Headward growth of chasmata by volatile outbursts, collapse, and drainage: Evidence from Ganges chaos, Mars, *Geophys. Res. Lett.*, 33, L18203, doi:10.1029/2006GL026275.

Rudoy, A., 1998. Mountain ice-dammed lakes of southern Siberian and their influence on the development and regime of the intracontinental runoff systems of North Asia in the late Pleistocene. Benito, G., Baker, V.R., Gregory, K.J. (Eds.), *Palaeohydrology and Environmental Change*, Wiley, Chichester, pp. 215-234.

Saunders, S. R., 1979. *Geologic map of the Margaritifer Sinus Quadrangle of Mars*: USGS Map I-1144, MC-19.

Smith, D.G., Fisher, T.G., 1993. Glacial Lake Agassiz – the northwest outlet and paleoflood. *Geology* 21 (1), 9-12.

Smith, D. E., Zuber, M. T., Frey, H. V., Garvin, J. B., Head, J. W., Muhleman, D. O., Pettengill, G., H., Phillips, R. J., Solomon, S. C., Zwally, H. J., Banerdt, W. B., Duxbury, T. C., 1998.

Topography of the northern hemisphere of Mars from the Mars Orbiter Laser Altimeter. *Science* 279, 1686–1692.

Sotin, C. and 25 co-authors, 2005. Release of volatiles from a possible cryovolcano from near-infrared imaging of Titan. *Nature* **435**, 786–789.

Starkel, L., 1995. Introduction to global palaeohydrological changes. In Gregory, K.J., Starkel, J., Baker, V.R. (Eds.), *Global Continental Palaeohydrology*, Wiley, Chichester, 1–20.

Stofan, E.R. and 37 co-authors, 2007. The lakes of Titan. *Nature* 445 (7123), 61–64.

Tanaka, K. L. 1986. The stratigraphy of Mars. *J. Geophys. Res.* 91, 139–158.

Tanaka, K.L., Chapman, M.G., 1990. The relation of catastrophic flooding of Mangala Valles, Mars, to faulting of Memnonia Fossae and Tharsis volcanism. *J. Geophys. Res.* 95, 14,315–14,323.

Tobie, G., Lunine, J.I., Sotin, C., 2006. Episodic outgassing as the origin of atmospheric methane on Titan. *Nature* 440, 61–64. doi:10.1038/nature04497.

Tokano, T., McKay, C.P., Neubauer, F.M., Atreya, S.K., Ferri, F., Fulchignoni, M., Niemann, H.B., 2006. Methane drizzle on Titan, *Nature* 442, 7101, 432–435. doi:10.1038/nature04948.

Tomasko, M.G., and 39 colleagues (2005). Rain, winds, and haze during the Huygens probe's descent to Titan's surface. *Nature* **438**, 765–778.

Tómasson, H. 1996. The jökulhlaup from Katla in 1918. *Annals of Glaciology* **22**, 249–254.

Waite, J.H., Young, D.T., Cravens, T.E., Coates, A.J., Crary, F.J., Magee, B., Westlake, J., 2007. The Process of Tholin Formation in Titan's Upper Atmosphere. *Science* 316 (5826), 870–875, doi:10.1126/science.1139727.

Waitt, R.B., 2002. Great Holocene floods along Jökulsá á Fjöllum, north Iceland. In: Martini, I.P., Baker, V.R., and Garzón, G. (Eds.), *Flood and Megaflood Processes and Deposits: Recent and Ancient Examples*. Spec. Publs int Ass. Sediment. 32, pp. 37–51.

Waythomas, C.F., Walder, J.S., McGimsey, R.G., Neal, C.A., 1996. A catastrophic flood caused by drainage of a caldera lake at Aniakchak Volcano, Alaska, and implications of volcanic hazards assessment. *Geol. Soc. Am. Bull.* 108(7), 861–871.

Wilson, L., Ghatan, G. J., Head, J. W., Mitchell, K. L., 2004. Mars outflow channels: A reappraisal of the estimation of water flow velocities from water depths, regional slopes, and channel floor properties. *Journal of Geophysical Research*, **109**, E09003, doi:10.1029/2004JE002281.

Wood, S.H., Clemens, D.M., 2002. Geologic and tectonic history of the western Snake River Plain, Idaho and Oregon. In *Tectonic and Magmatic Evolution of the Snake River Plain Volcanic Province. Idaho Geological Survey Bulletin 30*, ed. B. Bonnicksen, C.M. White and M. McCurry. Moscow, ID: Idaho Geological Survey Press, pp. 69-103.